GEOLOGICA CARPATHICA, OCTOBER 2021, 72, 5, 361–372 https://doi.org/10.31577/GeolCarp.72.5.1

U–Pb zircon ages from Permian volcanites of the Čierna Hora Mts. (Western Carpathians, Slovakia): Regional tectonic implications

ANNA VOZÁROVÁ[1,✉], NICKOLAY RODIONOV[2], KATARÍNA ŠARINOVÁ[1] and JOZEF VOZÁR[3]

[1]Comenius University in Bratislava, Faculty of Natural Sciences, Department of Mineralogy, Petrology and Mineral Resources, Mlynská dolina, Ilkovičova 6, 842 15 Bratislava, Slovakia; ✉vozarova@fns.uniba.sk, katarina.sarinova@uniba.sk
[2]Centre of Isotopic Research, A. P. Karpinsky Russian Geological Research Institute (FGBU «VSEGEI»), Sredny prospekt 74, 199 106 St.-Petersburg, Russia; Nickolay_Rodionov@vsegei.ru
[3]Earth Science Institute of the Slovak Academy of Sciences, Dúbravská cesta 9, 840 05 Bratislava, Slovakia; jozef.vozar@savba.sk

(Manuscript received May 6, 2021; accepted in revised form August 6, 2021; Associate Editor: Igor Broska)

Abstract: U–Pb dating of magmatic zircons from the Permian meta-andesites of the Čierna Hora Mts. yielded the Concordia ages of 267.0±1.5 Ma, which correspond to the Guadalupian Epoch in the time span of the Wordian Stage. The sequence was correlated with the Northern Veporic Permian rocks from the Čierťaž Mts. From the geochemical point of view, the studied volcanic rocks belong to a peraluminous calc-alkaline magmatic suite, linked to the post-collisional lithospheric extension. Lithosphere extension and attenuation will promote upwelling of hot asthenosphere. In this context, the calc-alkaline affinity may result through extensive crustal contamination of basaltic magma. Continuous extensional setting, succeeded by overheating is indicated by the newly formed zircon rims of 252.2±3.2 Ma age at the edges of the Wordian zircon grains. The Neoproterozoic (618±8 Ma) and Paleoproterozoic (2080±13 Ma) ages were found within the xenocrystic cores in the studied magmatic zircon grains. The presented xenocrystic zircon ages indicate derivation from the Variscan basement rocks with reworked fragments of Cadomian crust.

Keywords: SHRIMP zircon dating, Central Western Carpathians, Guadalupian volcanism, extensional setting.

Introduction

During the Alpine orogeny, relics of the Permian sedimentary basin fillings were incorporated into most of the Western Carpathian Alpine tectonic units, together with the preserved fragments of synsedimentary volcanic rocks in some places. Since the Permian sediments in the Western Carpathians are represented by the typical continental "red-beds", overlying the bedrock of the crystalline basement or Carboniferous sequences and underlying the Lower Triassic sediments, there was no general doubt about the Permian age of the associated volcanic rocks. However, a more accurate age classification of synsedimentary volcanism within the Permian Period remains a problem, as the associated sediments do not provide sufficient biostratigraphic data on their age. Therefore, in recent decades, attention has been focused on radiometric age dating of volcanics, which also brought new evidence for a more accurate determination of the evolution of Permian sedimentary basins in the Western Carpathians. The beginning of the Permian volcanic activity in the Western Carpathians was documented by the reworked Cisuralian as well as the older Kungurian and Asselian–Sakmarian magmatic ages (zircon SHRIMP ages: 281±6 Ma, Vozárová et al. 2013; 298–293 Ma, Vozárová et al. 2018, 2019a) within detrital zircon assemblages in the associated sediments. It should be noted that the Kungurian age is the most documented age within the Western Carpathians Permian volcanic rocks. However, the Guadalupian magmatic zircon ages were gradually detected. The summary of the Permian volcanic rock ages is given in Table 1.

The obtained zircon age data confirm the multistage Variscan post-orogenic and post-collisional tectonic regime for the genesis of the Permian volcanism in the Western Carpathians. It continued until the Lopingian/Lower Triassic in some places, as is documented by the Re–Os molybdenite ages (257±3 and 256±4 Ma, Kohút et al. 2013) and zircon SHRIMP age (251±4 Ma, Vozárová et al. 2015) from the Northern Gemeric Unit.

In an effort to complete the age data on the Permian volcanism in the Western Carpathians, magmatic zircons from the Permian volcanic body of the Čierna Hora Mts. were analysed (Fig. 1). It is one of the easternmost occurrences of the crystalline basement together with its Permian envelope in the Western Carpathians.

Geological backgrounds

The Čierna Hora Mts. entire area is composed mainly of the crystalline rock complexes and their Late Paleozoic–Mesozoic envelope sequences (Fig. 1) which are generally correlated with the Veporic Unit (in Polák & Jacko 1996; Polák et al. 1997). Expected Early Paleozoic age (Jacko 1978, 1985) results from a model age of lead from hydrothermal

Table 1: Summary of zircon magmatic ages in the Western Carpathians Permian volcanic rocks.

Age data in Ma	Method	Location	Authors
273±6 *279±4*	$^{206}Pb/^{238}U$ zircon SHRIMP	Northern Veporic Unit	Vozárová et al. 2016
278±11	conv. multi-grain zircon	Northern Veporic Unit	Kotov et al. 1996
272±3 *275±3*	$^{206}Pb/^{238}U$ zircon SHRIMP	Northern Gemeric Unit	Vozárová et al. 2012
269±7 *251±4*	$^{206}Pb/^{238}U$ zircon SHRIMP	Northern Gemeric Unit	Vozárová et al. 2015
278±11	Th–U–Pb monazite	Northern Gemeric Unit	Rojkovič & Konečný 2005
257±3 *256±4*	Re–Os molybdenite	Northern Gemeric Unit	Kohút et al. 2013
273±3 *275±3*	$^{206}Pb/^{238}U$ zircon SHRIMP	Southern Gemeric Unit	Vozárová et al. 2009a
276±25	Th–U–Pb monazite	Southern Gemeric Unit	Vozárová et al. 2008
266±2	$^{206}Pb/^{238}U$ zircon SHRIMP	Bôrka Nappe Meliatic Unit	Vozárová et al. 2012
273±2	$^{206}Pb/^{238}U$ zircon SHRIMP	Bôrka Nappe Meliatic Unit	Vozárová et al. 2019b
263±3	$^{206}Pb/^{238}U$ zircon SHRIMP	Northern Veporic Unit	Vozárová et al. 2020
260±1 *259±3*	$^{206}Pb/^{238}U$ zircon SHRIMP Th–U–Pb monazite	Tatric Unit	Pelech et al. 2017
262±2 *266±2*	U–Th–Pb SIMS	Infratatric Unit	Putiš et al. 2016
267±2 *263±2* *269±2*	U–Th–Pb SIMS	Muráň Nappe Silicic Unit	Ondrejka et al. 2018
263±3.5	Th–U–Pb monazite	Muráň Nappe Silicic Unit	Demko & Hraško 2013

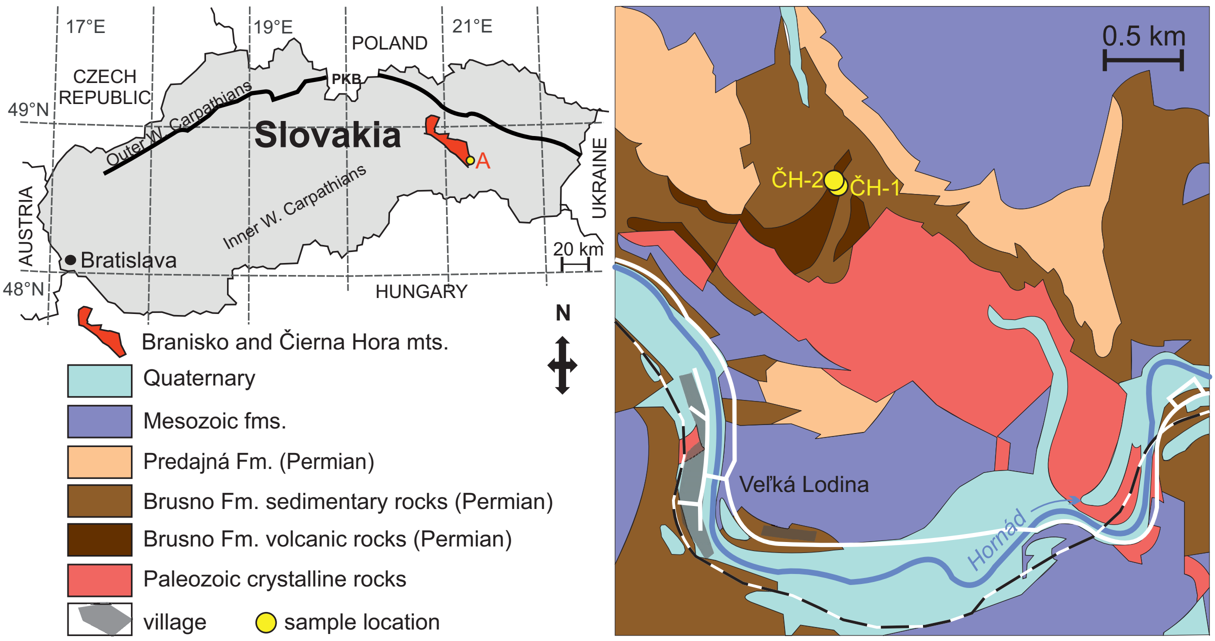

Fig. 1. Excerpts of details from the Geological map Branisko and Čierna Hora Mts., 1:50,000 (modified after Polák & Jacko 1996), showing localities of the studied samples.

redistributed galenite (370–376 Ma, Jacko & Baláž 1993). Clear dynamometamorphic reworking is assumed during Late Variscan movements, documented by $^{40}Ar/^{39}Ar$ dating of metamorphic muscovite (333–311 Ma, Dallmayer in Polák et al. 1997), as well as the presence of blastomylonite pebbles within the overlying Permian conglomerates. The Čierna Hora Mts. crystalline basement is one of the maxima retrograde tectonically reworked segments in the crystalline basements of the Central Western Carpathians. Three lithostratigraphic units, the lower Lodina Complex, the middle Miklušovce Complex and the upper Bujanová Complex, were defined by Jacko (1985) within these crystalline basement rocks.

In general, they consist of complexes in varying degrees of tectonized gneisses, amphibolites and migmatites into which Variscan granitoids have been intruded. The mutual contact of these complexes is tectonic, stressed by the coarse zones of phylonites or tectonic breccia. According to Jacko's interpretation, the genesis of these tectonic zones is poly-staged, starting with the Late Variscan events, through the Cretaceous nappe stacking of the Carpathian units to the post-Paleogene formation of regional NE-SE fault zones and large-scale uplifts/subsidences (e.g., Jacko & Rajlich 1973; Jacko & Sasvári 1990; Jacko et al. 1995, 2021 and references therein).

Permian sediments in the area of the Čierna Hora Mts. are preserved mainly at the NE and SW edges of the crystalline basement. No biostratigraphic dating has been made so far. Their direct contact with the underlying crystalline complexes but then again also with the overlying Mesozoic sedimentary sequences is usually tectonized. In general, Permian rock complexes are tectonically deformed and recrystallized, especially along the Alpine shear zones.

Permian sediments in the Čierna Hora Mts. are represented by the continental, predominantly coarse-grained metasandstones and metaconglomerates which, based on their lithological composition, were correlated with the envelope sequence of the Northern Veporic Unit (Vozárová & Vozár 1988; Polák et al. 1997). In the Čierna Hora Mts., as in the Northern Veporicum (Vozárová 1979), two lithostratigraphic units were separated, the Brusno and Predajná formations.

The Brusno Formation sequence consist of small- to medium-grained metaconglomerates, alternating with very coarse- and coarse-grained metarkoses and feldspar metagreywackes, with scarce intercalations of sandy shales. Sediments have structural features characteristic of gravelly and sandy alluvium of braided rivers. Their mineral composition reflects the petrological character of the immediate basement rocks. The detrital component is dominated by quartz (52 %), plagioclase (24 %) and alkaline feldspar (14 %), with a lower amount of detrital mica (4 %) and fragments of synsedimentary volcanic rocks (6 %) (average calculated from 9 modal analyses). The pebble material in metaconglomerates consists of quartz, granitoids and fragments from synsedimentary volcanic rocks. An integral part of the Brusno Formation is the dacite-andesite volcanic horizon, from which the ages of igneous zircons included in this study were dated.

In the complicated Alpine tectonic structure of the Čierna Hora Mts., the Predajná Formation metasediments are usually significantly tectonically reduced. They consist of a cyclically arranged set of variegated metasandstones and shales with intercalations of polymictic metaconglomerates. Fragments of various types of crystalline schists, metaquartzites, volcanics, granitoid rocks and quartz are significant within the pebble material of metaconglomerates. The associated metasandstones correspond to lithic metagreywackes, with the following mineral components: quartz (55 %), plagioclase (8 %), alkaline feldspar (7 %), detrital mica (6 %), metamorphic rock fragments (12 %) and volcanic rock fragments (11 %) (average from four samples).

Analytical methods

Two samples were taken from the Permian volcanic rocks for petrological and geochemical characteristics (samples *ČH-1, ČH-2*), of which one sample (*ČH-1*) has been processed for magmatic zircon dating. Their location is as follows: Sopotnica valley, N from Velká Lodina village. GPS coordinates: sample *ČH-1*: 48°52.682'N, 21°09.924'E; sample *ČH-2*: 48°52.735'N, 21°09.916'E.

The rock-forming minerals were studied by the electron microprobe JEOL JXA 8530OF, in the Laboratory of Electron Microanalysis (EMPA) of the Earth Science Institute of the Slovak Academy of Sciences, division Banská Bystrica. Zircons have been extracted from the rocks by standard grinding, heavy liquid and magnetic separation analytical techniques. The internal structure of individual zircon crystals was examined with cathodoluminescence (CL) imaging by SEM (CamScanM2500 Oxford Instruments). In situ U–Pb analyses were performed using a Sensitive High-Resolution Ion Microprobe (SHRIMP-II) at the Centre of Isotopic Research (CIR) in the A.P. Karpinsky Russian Geological Institute (VSEGEI), by applying a secondary electron multiplier in peak-jumping mode, based on the procedure described by Williams (1998). Primary beam diameter allowed the analysis an area of ca. 25×20 µm. CL, BSE and optical (transmitted light) imaging was applied to reveal the internal and surface features that were used to choose the position of analytical spots on the mostly homogeneous inclusion-free parts of individual zircon grains. The 80 µm wide ion source slit, in combination with a 100 µm multiplier slit, allowed for the mass-resolution M/ΔM≥5000 (1 % valley); hence, all the possible isobaric interferences were resolved. The following ion species were measured in the sequence: $^{196}(Zr_2O)$–^{204}Pb–background(ca.$^{204.5}$AMU)–^{206}Pb–^{207}Pb–^{208}Pb–^{238}U–^{248}ThO–^{254}UO. At least 4 mass-spectrums were acquired for each analysis. Zircon Temora-2 (Black et al. 2004) was measured as the main reference material (RM): one analysis per every four analyses of unknowns to obtain their U/Pb ratios. Zircon 91500 (Wiedenbeck et al. 1995) was used as a concentration RM. The obtained results were processed by the SQUID v1.12 (Ludwig 2005) and ISOPLOT/Ex 3.75 (Ludwig 2012) software, with decay constants recommended by Steiger & Jäger (1977), including modern corrections such as Hiess et al. (2012). Common lead correction was done on the basis of the measured $^{204}Pb/^{206}Pb$ ratio. The ages given in this text, if not additionally specified, are $^{207}Pb/^{206}Pb$ for zircon older than 1.0 Ga, and $^{206}Pb/^{238}U$ for those younger than 1.0 Ga. The degree of discordance was calculated according to the following formula: %D=100*[(Age 207–235)/(Age 206–238)–1]. The uncertainties are quoted at standard deviation level (1s, i.e. 68.3 % confidence) for individual points and at 2s level in the Concordia diagram, for the Concordia ages or any previously published ages discussed in the text. Only analyses that overlap Concordia line within individual uncertainties were used for concordant-age calculation. The time-scale calibration of the International Chronostratigraphic Chart v2021-05 was used to compare geochronological data from detrital zircons with fossil-bearing sedimentary units and tectono–thermal events.

The rock samples have been analysed for whole rock chemical composition, rare earth and trace elements in the Bureau Veritas Commodities Canada Ltd. (former ACME Analytical Laboratories Ltd., Canada). Following a lithium metaborate/tetraborate fusion and dilute nitric digestion, major elements were determined by inductively coupled plasma (ICP-ES) and trace and rare elements (REE) by inductively coupled plasma mass spectrometry (ICP-MS). The analytical accuracy is estimated to be within a 0.01 % error (1σ, relative) for major elements, and within a 0.1–0.5 ppm error range (1σ, relative) for trace elements and 0.01–0.05 ppm for REEs.

Characteristics of samples

Petrology

The considered volcanic rocks are typical with a dark-violet colour and aphanitic or fine-porphyritic structure. They were affected by Alpine dynamic metamorphism, where foliation obliterated the initial rock texture. The micro-porphyritic texture being dominated by phenocrysts of quartz, plagioclase and biotite (Fig. 2A, B). Strong decomposed amphiboles are rare. Phenocrysts make up about 20–30 % of the total rock volume. The fine-grained foliated and recrystallized matrix aggregate is dominant.

Individual beta-quartz phenocrysts have embayed margins and are wrapped by fine aggregates of chlorite and opaque minerals. Quartz crystals are mostly anhedral, assumed due to magmatic resorption. They are also extensively fractured with slight oscillatory zoning in some places, often truncated by resorption surfaces. Resorbed and embayed quartz crystals with dissolution surfaces are found throughout the whole texture.

Plagioclases have undergone complex alteration in both the magmatic and post-magmatic, hydrothermal stages. Only the contours of the original phenocrysts are preserved, and are additionally pressure deformed along the foliation surfaces. In the first place, they were replaced from the edges to the centre by potassium feldspar. The central parts of the original plagioclases were albitized and sericitized, with isolated inclusions of calcite (Fig. 2C).

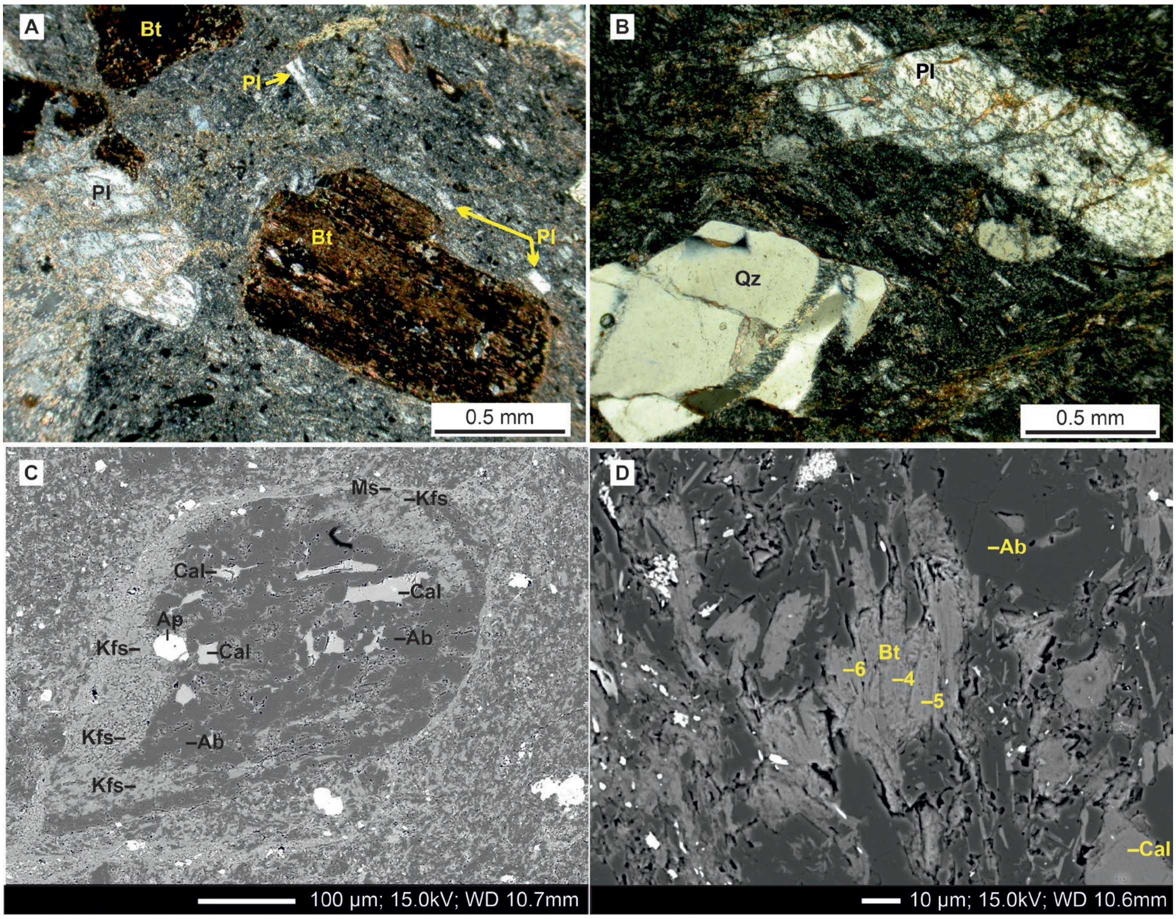

Fig. 2. Photomicrographs of the Čierna Hora Mts. metaandesites: **A** — Sample *ČH-1*, deformed and altered biotite and plagioclase crystals; slightly oriented and recrystallized groundmass with plagioclase lathes; **B** — Sample *ČH-2*, fragmented quartz and plagioclase crystals with recrystallized groundmass; **C** — Sample *ČH-2*, BSE image of strongly altered and deformed plagioclase crystal; **D** — Sample *ČH-1*, BSE image relic of deformed and altered biotite phenocryst.

Phenocrysts of biotites are almost completely decomposed (Fig. 2A). It is preserved only in relics (Fig. 2D). Along the cracks it is converted into an aggregate of chlorite, sericite and Fe–Ti oxides. They contain inclusions of apatite, zircon, titanite and Ti-magnetite. Electron-microprobe analyses (Table 2) indicate a relatively homogeneous chemical composition of the biotite relics, belonging to the annite–phlogopite series (Fig. 3). Phlogopites have *mg#* [=100.Mg/(Mg+Fe_T) in mols] ranging from 68 to 74, and Cr_2O_3 concentrations mostly between 0.01 and 0.17 wt. %. In only one analysis do they reach 1.24 wt. %. Exceptions are relatively higher concentrations of BaO, most often in the range of 0.10 to 0.71 wt. %, remarkably up to 2.45 wt. %. Relatively variable but in some analyses comparatively high TiO_2 contents were found, ranging from 0.89 to 6.15 wt. % (Table 2).

Recrystallized groundmass consists of fine-grained, considerably preferred aggregate sericite, Fe-Ti oxide/hydroxides, calcite, albite, quartz and scarce chlorite. Fine needles of rutile and crystals of apatite are frequent. Laths and needles of plagioclases are replaced by albite and sericite. Magnetite and ilmenite were detected as primary magmatic phases, either as inclusions in the mafic phenocrysts or as individual grains in the groundmass.

Geochemistry

Major- and trace elements including REEs are given in Table 3. The studied rocks underwent a significant degree of metasomatism and secondary alteration. This is reflected by LOI values, which vary from 3.1–2.5 wt. %. Immobile trace elements such as high field strength elements (HFSE) and rare elements (REEs) have been used to classify rocks and monitor magmatic affinities. The studied volcanic rocks belong to the group of andesites of the sub-alkaline magmatic series according to the Zr/Ti versus Nb/Y (proxy diagram after Winchester & Floyd 1977 modified after Pearce 1996, 2014) (Fig. 4A). This is clearly documented by the 0.54 and 0.55 Nb/Y ratio values, as well as the 0.043 and 0.045 Zr/Ti ratio values, respectively. Major elements geochemical classification of the Čierna Hora andesitic rocks shows the following

Table 2: Representative microprobe analyses of biotite phenocrysts (*calculated to stechiometry).

sample analyse	ČH-2 1	ČH-2 2	ČH-2 3	ČH-2 4	ČH-2 5	ČH-2 6	ČH-1 4	ČH-1 5	ČH-1 6	ČH-1 11	ČH-1 12	ČH-1 13
SiO_2	40.64	39.27	39.42	41.40	41.48	41.18	40.60	41.30	40.93	38.75	39.04	38.33
TiO_2	3.73	4.57	6.13	2.75	1.04	0.89	1.37	1.22	1.36	4.90	5.20	4.12
Al_2O_3	12.60	13.16	11.92	12.32	13.72	14.13	13.36	13.61	13.60	13.19	13.33	14.89
Cr_2O_3	0.00	0.00	0.02	0.00	1.24	0.17	0.04	0.03	0.03	0.00	0.01	0.00
FeO	13.39	14.18	12.43	12.09	11.05	11.52	12.67	13.01	12.04	15.39	16.02	13.15
MgO	15.98	14.50	16.11	17.51	17.57	17.76	16.88	17.46	16.64	13.63	12.79	14.04
MnO	0.23	0.26	0.16	0.18	0.21	0.18	0.22	0.22	0.13	0.24	0.27	0.30
BaO	0.61	2.45	0.71	0.19	0.41	0.05	0.09	0.53	0.10	0.38	0.65	0.42
CaO	0.03	0.01	0.01	0.01	0.04	0.03	0.09	0.02	0.03	0.05	0.07	0.07
K_2O	10.03	9.88	9.69	10.00	9.49	9.65	9.90	10.13	10.05	9.96	9.85	9.57
Na_2O	0.02	0.03	0.00	0.02	0.03	0.03	0.03	0.00	0.05	0.01	0.13	0.17
Cl	0.10	0.12	0.09	0.13	0.01	0.02	0.02	0.02	0.02	0.13	0.16	0.13
F	0.55	0.37	0.55	0.71	0.62	0.60	0.55	0.70	0.59	0.16	0.37	0.00
Total	97.90	98.80	97.23	97.29	96.91	96.20	95.80	98.24	95.55	96.80	97.88	95.17
Si	2.960	2.886	2.874	3.005	2.999	2.992	2.991	2.983	3.012	2.877	2.884	2.851
^{T}Al	1.040	1.114	1.024	0.995	1.001	1.008	1.009	1.017	0.988	1.123	1.116	1.149
^{T}Fe	0.000	0.000	0.102	0.000	0.000	0.000	0.000	0.000	0.000	0.000	0.000	0.000
Sum T	4.000	4.000	4.000	4.000	4.000	4.000	4.000	4.000	4.000	4.000	4.000	4.000
Al	0.041	0.026	0.000	0.059	0.168	0.203	0.150	0.141	0.191	0.031	0.045	0.157
Ti	0.204	0.253	0.336	0.150	0.057	0.049	0.076	0.066	0.075	0.274	0.289	0.231
Fe	0.815	0.872	0.656	0.734	0.668	0.700	0.780	0.786	0.741	0.956	0.990	0.818
Mg	1.734	1.589	1.751	1.895	1.893	1.924	1.853	1.879	1.826	1.509	1.408	1.557
Mn	0.014	0.016	0.010	0.011	0.013	0.011	0.014	0.013	0.008	0.015	0.017	0.019
Cr	0.000	0.000	0.001	0.000	0.071	0.010	0.002	0.001	0.001	0.000	0.000	0.000
Ni	0.000	0.000	0.000	0.000	0.000	0.000	0.000	0.000	0.000	0.000	0.000	0.000
Sum M	2.809	2.755	2.754	2.848	2.869	2.896	2.876	2.888	2.842	2.785	2.749	2.782
Ca	0.002	0.000	0.001	0.001	0.003	0.002	0.007	0.001	0.002	0.004	0.005	0.005
Ba	0.017	0.071	0.020	0.005	0.012	0.001	0.003	0.015	0.003	0.011	0.019	0.012
K	0.932	0.927	0.902	0.926	0.875	0.895	0.930	0.933	0.943	0.944	0.928	0.908
Na	0.002	0.004	0.001	0.003	0.004	0.004	0.004	0.000	0.007	0.002	0.019	0.024
Sum I	0.954	1.001	0.923	0.934	0.895	0.902	0.944	0.950	0.956	0.960	0.971	0.949
F	0.128	0.087	0.128	0.164	0.141	0.138	0.127	0.159	0.137	0.038	0.087	0.000
Cl	0.013	0.015	0.012	0.016	0.001	0.002	0.002	0.003	0.002	0.017	0.020	0.016
OH*	1.860	1.899	1.861	1.820	1.858	1.860	1.870	1.838	1.861	1.945	1.892	1.984
I charge	0.973	1.072	0.944	0.940	0.910	0.906	0.954	0.966	0.961	0.975	0.995	0.967

compositional parameters (after Frost et al. 2001): molar alumina saturation index (ASI)=Al_2O_3/CaO+Na_2O+K_2O and modified alkali lime index (MALI)=(Na_2O+K_2O)−CaO. The studied andesites correspond to peraluminous calc-alkaline magmatic suite. The Fe numbers (FeO_t/FeO_t+MgO=0.63 and 0.70), correlated with amount of SiO_2 (60–63 wt. %), make these rocks to magnesian, although near the border with ferroan magmatites. Their calc-alkaline magmatic trend is also documented on the basis of Zr/Y ratios (after MacLean & Barret 1993), with values of 8.8 and 9.1.

Generally, the values of ΣREE correspond to 236 and 218 ppm which is relatively high. The volcanics have identical REE partition patterns (normalized to chondrite after Sun & McDonough 1989; Fig. 4B), with light rare earth element (LREE) enrichments (La_N/Sm_N=3.95 and 3.98) and slight Eu negative anomalies (Eu/Eu*=0.82 for both samples). The $(La/Yb)_N$ ratios, within 14.33 and 14.38 respectively, also indicate a proportional depletion of heavy REE (HREE), with no significant HREE fractionation.

Trace element concentrations normalized to composition of upper continental crust (UCC) (after McLennan 2001) show distinctive depletion in Sr (Fig. 4C) and a relatively higher enrichment in Cs, Rb, Ba relative to Th, U and K. Compared to UCC the analysed volcanic rocks display a slight enrichment in LREE, middle REE and P. Conversely, the contents of Th, Ta, Nb, Zr, Ti and HREE they are almost the same as in the UCC.

Zircon age dating

Zircon grains are mostly medium in size (100–200 µm). Generally, zircons are prismatic and colourless or pink. The majority of zircon grains display magmatic oscillatory

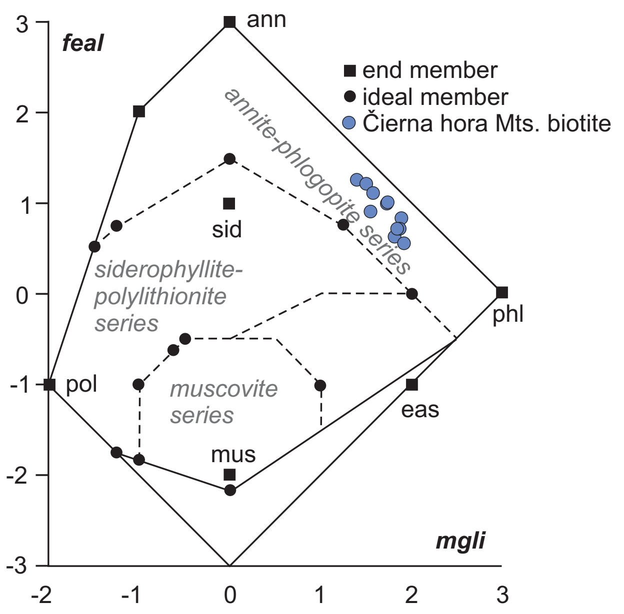

Fig. 3. Classification ***mgfli/feal*** diagram of biotites (according to Tischendorf et al. 2007).

growth zoning (regular or irregular), concentric and less of marginal sector type. Cathodoluminescence (CL) images show that some grains are composite, with inherited cores surrounded by a new growth zonation (Fig. 5). Commonly,

Table 3: Representative major-, trace elements, including REE in the Čierna Hora Mts. meta-andesites (b.d.l. – sample below detection limit; all Fe measured as Fe_2O_3).

Sample		ČH-1	ČH-2
SiO_2	wt. %	60.13	62.93
Al_2O_3		15.84	15.88
Fe_2O_3		5.12	4.69
MgO		2.73	1.82
CaO		2.21	1.53
Na_2O		4.45	3.94
K_2O		4.92	5.29
TiO_2		0.83	0.81
P_2O_5		0.28	0.27
MnO		0.08	0.05
Cr_2O_3		0.018	0.016
Ni	ppm	28	44
Sc	ppm	16	15
LOI	wt. %	3.1	2.5
Sum	wt. %	99.85	99.86
Ba	ppm	1381	1501
Be		2	3
Co		18.4	12.6
Cs		18.8	11.7
Ga		17.2	17
Hf		5.7	5.5
Nb		13.3	13.3
Rb		190.5	190
Sn		3	3
Sr		103.6	89.2
Ta		1	0.9
Th		11.4	11.1
U		3.4	3.4
V		124	120
W		1.8	2.2
Zr		218.9	219.4
Y		24.8	24
La		50.2	46.8
Ce		100.3	92.4
Pr		12.03	11.04
Nd		46.3	41.9
Sm		7.93	7.34
Eu		1.67	1.54
Gd		6.19	5.78
Tb		0.81	0.8
Dy		4.45	4.28
Ho		0.85	0.87
Er		2.58	2.48
Tm		0.35	0.34
Yb		2.38	2.21
Lu		0.34	0.34
C_{total}	wt. %	0.38	0.24
S_{total}	wt. %	b.d.l.	b.d.l.
Eu/Eu*		0.73	0.72
$(La/Sm)_N$		3.95	3.98
$(La/Yb)_N$		14.33	14.40
Zr/Ti		0.04	0.04
FeO/(FeO+MgO)		0.63	0.70

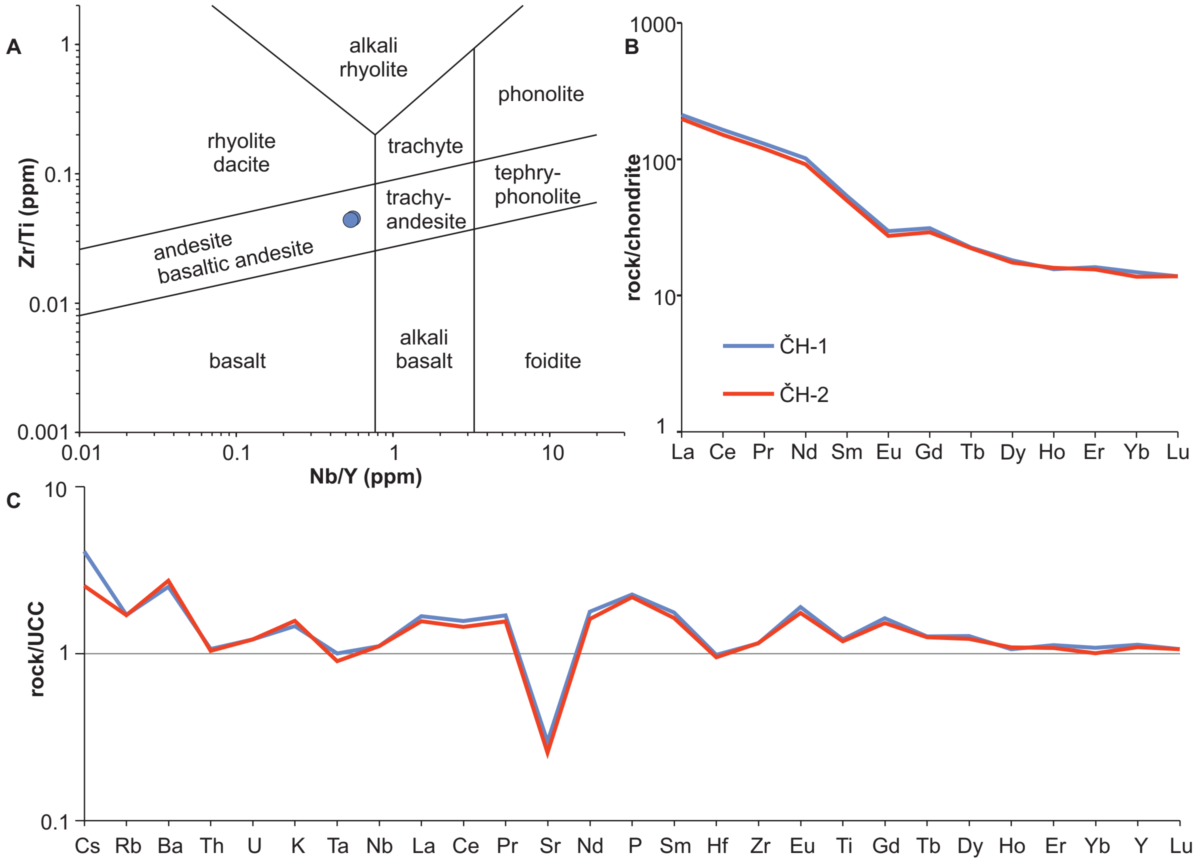

Fig. 4. A — Classification of the Čierna Hora Mts. Permian volcanic rocks based on Zr/Ti vs. Nb/Y diagram after Winchester & Floyd (1977) revised by Pearce (1996); **B** — Chondrite-normalized REE distribution of the studied volcanic rocks. Chondrite normalizing values after Sun & McDonough (1989); **C** —Upper Continental Crust normalized incompatible element's diagram of the studied samples. Normalizing values after McLennan (2001).

Fig. 5. Cathodoluminescence zircon images with indication of the age data (in Ma). The age data correspond to $^{238}U/^{206}Pb$ ages up to 1.0 Ga and to $^{206}Pb/^{207}Pb$ age data for >1.0 Ga.

the regular growth zoning is interrupted by the textural disconformities.

Out of the total number of 18 zircon grains, 20 spots were analysed (Table 4). Zircon ages, obtained from 15 grains, both from edges and central parts, yield $^{206}Pb/^{238}U$ concordant ages in the range of 262–276 Ma, with the Concordia age of 267.0±1.5 Ma (95 % confidence, decay-constant errors included; MSWD=0.28; Probability=0.60) (Fig. 6). This age clearly corresponds to the Guadalupian, just inside of the Wordian Stage, and represents the magma crystallization age of the Čierna Hora Permian volcanic rocks. Th–U ratios, ranging from 0.09 to 0.96, suggest that felsic magma was the host for the zircon formation. Values of below 1 are typical for felsic origin (Wang et al. 2011). However, values approaching 1, although rare, do not rule out minor mafic influences.

Age data from the other two zircon edges displayed much younger ages, 252.0±2.4 and 252.3±2.4 Ma, with Concordia age 252.2±3.4 Ma (95 % confidence, decay-constant errors included; MSWD=0.17; Probability=0.68) (Fig. 6). Low values Th–U ratios (0.17 and 0.16) also indicate crystallization from the felsic melt. These age data indicate the highest Lopingian, up to the Permian/Triassic boundary. These young ages have

Table 4: U–Pb (SHRIMP) magmatic zircon age data from the sample ČH-1. Errors are 1-sigma; Pb_c and Pb* indicate the common and radiogenic portions, respectively. Error in Standard calibration was 0.35 % (not included in above errors but required when comparing data from different mounts). (1) Common Pb corrected using measured ^{204}Pb; (2) Common Pb corrected by assuming $^{206}Pb/^{238}U$–$^{207}Pb/^{235}U$ age-concordance. % Discordance is calculated from $^{207}Pb/^{235}U$ vs. $^{206}Pb/^{238}U$ ages.

Spot	$^{206}Pb_c$ %	U ppm	Th ppm	$^{232}Th/^{238}U$	$^{206}Pb^*$ ppm	(1) Age $^{206}Pb/^{238}U$	±	(2) Age $^{206}Pb/^{238}U$	±	(1) Age $^{207}Pb/^{206}Pb$	±	(1) Age $^{207}Pb/^{235}U$	±	Discor. %	(1) $^{207}Pb^*/^{206}Pb^*$	± %	(1) $^{207}Pb^*/^{235}U$	± %	(1) $^{206}Pb^*/^{238}U$	± %	err. corr.
1.1	0.13	581	524	0.93	49.9	613.8	5.9	613.3	6.0	636	28	618.5	7.6	0.8	0.0609	1.3	0.8390	1.6	0.0999	1.0	0.611
1.2	0.21	588	83	0.15	42.2	515.8	5.0	515.4	5.1	538	35	519.8	7.7	0.8	0.0582	1.6	0.6690	1.9	0.0833	1.0	0.533
2.1	0.28	946	183	0.20	34.4	266.5	2.6	266.3	2.7	286	44	268.4	5.1	0.7	0.0520	1.9	0.3026	2.2	0.0422	1.0	0.469
3.1	0.34	623	175	0.29	22.8	267.7	2.8	267.6	2.8	276	57	268.5	6.3	0.3	0.0518	2.5	0.3027	2.7	0.0424	1.1	0.394
4.1	0.37	650	606	0.96	23.6	265.3	2.9	265.2	2.9	280	56	266.9	6.3	0.6	0.0519	2.4	0.3006	2.7	0.0420	1.1	0.410
5.1	0.17	943	375	0.41	34.3	266.7	2.6	266.7	2.7	266	41	266.6	4.8	0.0	0.0516	1.8	0.3003	2.1	0.0422	1.0	0.492
6.1	0.39	634	260	0.42	23.4	269.8	2.8	270.0	2.8	237	59	266.5	6.5	−1.2	0.0509	2.6	0.3001	2.8	0.0427	1.1	0.381
7.1	0.36	686	180	0.27	25.0	267.3	2.9	267.3	2.9	262	55	266.7	6.2	−0.2	0.0515	2.4	0.3003	2.6	0.0423	1.1	0.413
8.1	0.20	1053	152	0.15	38.5	268.5	2.6	268.9	2.7	225	41	264.1	4.7	−1.6	0.0507	1.8	0.2971	2.0	0.0425	1.0	0.495
9.1	0.32	1487	225	0.16	51.1	252.0	2.4	252.0	2.5	251	38	251.9	4.3	0.0	0.0512	1.7	0.2816	1.9	0.0399	1.0	0.510
10.1	0.08	1325	116	0.09	49.7	275.5	3.9	275.8	4.0	240	32	271.8	4.8	−1.3	0.0510	1.4	0.307	2.0	0.0437	1.5	0.720
11.1	0.43	1034	377	0.38	37.9	268.5	2.7	268.6	2.7	259	48	267.6	5.4	−0.3	0.0514	2.1	0.3015	2.3	0.0425	1.0	0.437
11.2	0.07	1297	872	0.69	46.2	261.5	2.5	261.4	2.6	275	34	262.8	4.1	0.5	0.0518	1.5	0.2955	1.8	0.0414	1.0	0.561
12.1	0.50	1219	389	0.33	43.7	262.0	2.6	262.4	2.6	203	49	256.1	5.3	−2.2	0.0502	2.1	0.2869	2.3	0.0415	1.0	0.429
13.1	0.11	238	87	0.38	78.9	2104	19	2109	23	2080	13	2092.0	11.5	−0.6	0.1287	0.7	6.8480	1.3	0.3860	1.1	0.826
13.2	0.51	322	70	0.22	11.8	266.7	3.1	266.1	3.1	343	86	274.7	9.6	3.0	0.0533	3.8	0.3110	4.0	0.0422	1.2	0.297
14.1	0.47	510	157	0.32	18.7	268.0	3.0	268.1	3.1	249	71	266.0	7.7	−0.7	0.0512	3.1	0.2995	3.3	0.0425	1.2	0.349
14.2	0.27	879	507	0.60	31.9	265.7	2.7	265.3	2.7	317	47	271.0	5.5	2.0	0.0527	2.1	0.3059	2.3	0.0421	1.0	0.446
15.1	0.16	1774	286	0.17	60.9	252.3	2.4	252.1	2.4	277	40	254.7	4.5	1.0	0.0518	1.7	0.2851	2.0	0.0399	1.0	0.490
15.2	0.80	274	96	0.36	10.3	273.7	3.3	274.0	3.4	239	140	270.0	14.5	−1.3	0.0510	6.0	0.3050	6.1	0.0437	1.2	0.202

been found either at the edge of the grains (spot. 9.1, Table 4; Fig. 5), or lining the older Permian core, 273.7±3.3 Ma old (spots 15.1 and 15.2, Table 4; Fig. 5).

Among the studied zircons only two xenocrystic zircon grains were found. In the first case (spots 1.1 and 1.2, Table 4), a substantial part is formed by fine growth-zoned magmatic zircon with age of 613.3±6 Ma (Ediacaran), which was subsequently partially magmatically resorbed and grown up with a new zircon aged 515.8±5 Ma (Cambrian). The second xenocrystic grain emerges in the crystal core and is of a very old age, 2080±13 Ma (Paleoproterozoic). This old core is bordered by the newly-formed zircon, with fine growth zoning, and Permian age: 266.7±3.1 Ma (spots 13.1 and 13.2, Fig. 5).

Discussion

Geochemical characteristics, especially the ratio values Th/Yb (4.8–5.0), Ta/Yb (0.41–0.42) as well as Th/Ta (11.4–12.3) and Nb/Yb (5.6–6.0) indicate the approximation of the Čierna Hora volcanic rocks to the volcanics of an active continental margin (e.g., Pearce 1983; Gorton & Shandl 2000). Although the studied volcanic rocks have petrological and geochemical characteristics similar to those of subducted-related calc-alkaline suite, paleogeographic reconstruction seems to exclude direct relationship with subduction processes, temporal and spatial. In particular, they are associated with the huge mass of continental, predominantly arkose-feldspar greywacke metasediments. All the geological and tectonic evidence indicates their origin in an intra-continental extensional regime which was caused by the Late Paleozoic dextral transtensional tectonics triggered by the relative motion of Gondwana and Laurasia (Arthaud & Matte 1977; Vai 1991; Ziegler 1993). The Čierna Hora intermediate volcanic rocks show distinct similarities to average upper continental crust (UCC; Rudnick & Fountain 1995) and exhibit flat calc-alkaline signatures only with an insufficient impoverishment of Ta, Nb relative to UCC. These intermediate volcanic rocks were most likely derived from a partial melting of thermally weakened subcontinental lithospheric source that further ascended with significant crustal assimilation (e.g., Bonin 2004).

The detected U–Pb zircon age data classifies the Čierna Hora Mts. volcanic rocks to the mid-Permian magmatic event. The $^{206}Pb/^{238}U$ 267.0±1.5 Ma Concordia age, which is interpreted as the age of magma crystallization, was unambiguously determined by the zircon analysis (Fig. 6). This age clearly corresponds to Guadalupian, directly matching

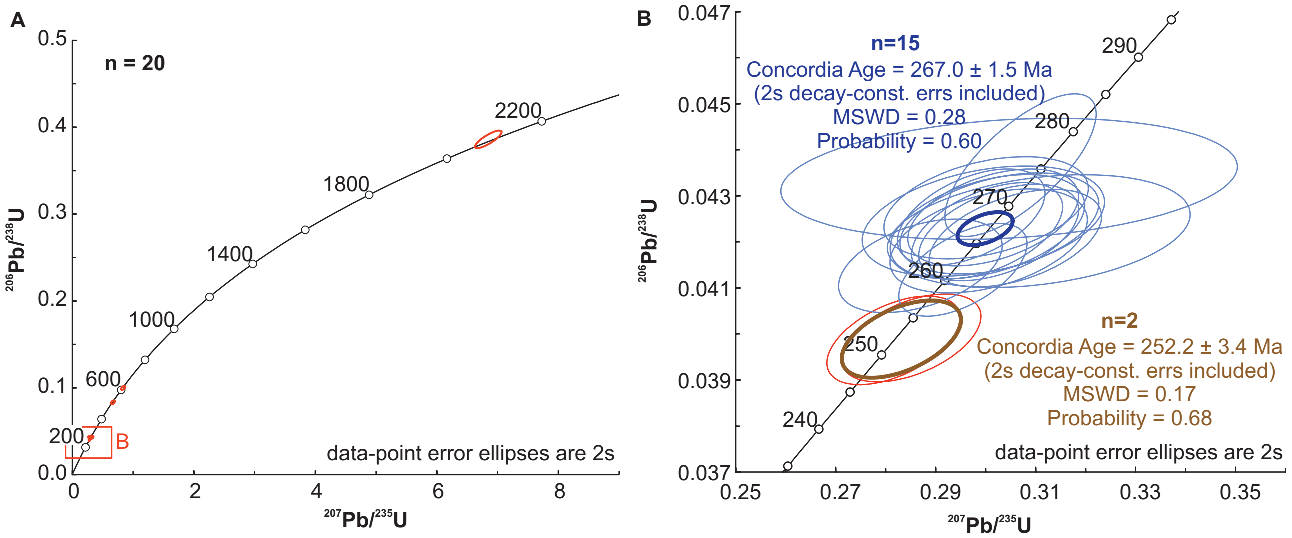

Fig. 6. Concordia plots of magmatic zircons from the *ČH-1* sample: **A** — Concordia plot for all magmatic and inherited zircons; **B** — Concordia age of the Čierna Hora volcanic rocks, indicating the magma crystallization age; selected sector of the Concordia for reheating age of 252.2±3.4 Ma.

the Wordian stage. The ages of 17 zircon spots define a weighted mean $^{206}Pb/^{238}U$ age of 264.7±3.2 Ma with an MSWD=5.2. The zircon ages from the Permian volcanites in the Čierna Hora Mts. could be compared with U–Pb zircon age data obtained from the Permian volcanic rocks in the Považský Inovec Mts. (266±2 and 262±2 Ma – Putiš et al. 2016; 260±1 Ma – Pelech et al. 2017), as well as from the Permian volcanics in the Muráň Nappe (263±2 and 269±2 Ma – Ondrejka et al. 2018 and Demko & Hraško 2013 – 263 ±3.5 Ma EMPA monazite ages) and from the Jasov Formation of the Bôrka Nappe (266±2 Ma – Vozárová et al. 2012) (Table 1). All these ages indicate the Guadalupian volcanic event, overwhelming mainly the Wordian and Capitanian Stages, in the range of ca. 260–268 Ma. This volcanic event is also equivalent to the II eruption phase of the Malužiná Formation andesite-basalts in the Hronicum Unit (Vozárová et al. 2018).

Very similar U–Pb zircon ages were determined in felsic volcanic rocks from Tisza Megaunit in Hungary, ranging from 260 to 267 Ma (LA-SF-ICP-MS; Szemerédi et al. 2020) and also from Apuseni Mts. (264–266 Ma, ID-TIMS; Pană et al. 2002) and from the Southalpine Unit, the Mid-Permian Bosen porphyry (e.g., Krainer 1993; Hubmann et al. 2014). Minor occurrences of Late Permian volcanic and volcaniclastic rocks (ages estimated from litho-biostratigraphy and other aspects) were found in the Lower-/Middle Austro-Alpine and Penninic nappe systems (Ebner in Vozárová et al. 2009b), connected with red-beds of the “Alpine Verrucano” facies.

So far U–Pb zircon dating in the Permian sequences of the Western Carpathians shows that the dominant phase of volcanic activity was in Kungurian, ranging from 273 to 279 Ma. Records of Asselian-Artinskian volcanic events are only indirectly derived from detrital zircon assemblages that were identified in the linked Permian sedimentary sequences, with the ages ranging from 281 to 299 Ma, (Vozárová et al. 2019a, 2018 in the Northern Gemericum and Hronicum sequences). It should be emphasized that the common feature of all Kungurian volcanites is their calc-alkaline chemical character and rhyolite-dacite composition. In the Western Carpathians, this calc-alkaline trend is characteristic also for the Guadalupian volcanites. The only exceptions are A-type rhyolites in the Silicic Unit (Muráň Nappe; Ondrejka et al. 2018) and tholeiitic trend of andesite-basalts in the Hronic Unit (Vozár 1997; Dostál et al. 2003). However, what is a substantial difference is a higher basic chemical composition most of the Guadalupian volcanites that are generally intermediate to basic, compared to the dominant Kungurian felsic volcanites.

The Mid-Permian timing of volcanism is coeval with magmatic events, which were described during recent decades in the Western Carpathians (for summary Ondrejka et al. 2021; Villaseñor et al. 2021), as well as in the Eastern Alps (e.g., Yuan et al. 2020).

Particular attention should be paid to 252.3±3.4 Ma zircon ages found in growth lamellae at the edges of magmatic zircons (Figs. 5, 6). Such young Permian ages were so far found only in the Permian volcanites of the Northern Gemeric Unit (251±4 Ma, Vozárová et al. 2015).

It follows that those three stages of volcanic activity can be indicated within the Permian sequences in the Western Carpathians, each of them associated with the thermal effects induced by lithospheric thinning and rifting. Cisuralian volcanic phases can be associated with post-orogenic transpressional/transtensional movements of the final stages of the Variscan orogeny. In the Western Carpathians, they include the dominant Kungurian volcanic association, and also the Asselian–Artinskian volcanic activity, which can be indicated from the detrital zircon ages in associated Permian sediments.

The Guadalupian volcanic event (Wordian-Capitanian), which also includes the occurrences in the Čierna Hora Mts., indicates the process of extension succeeding the post-collision stage, which continued in the latest Lopingian (Changhsingian) and further in the Triassic. It also means the beginning of the Alpine orogenic cycle.

Conclusions

U–Pb zircon ages from the intermediate Permian volcanic rocks in the territory of the Čierna Hora Mts. confirmed the Mid-Permian extensional tectonic setting succeeding the beginning of the Alpine orogenic cycle. The Concordia age of 267.0±1.5 Ma, documented from 15 spots of magmatic zircons, clearly proved magma crystallization age. Significant reheating at 252.2±3.4 Ma associated with Permian–Triassic extensional movements was recognized in marginal parts of some zircon grains.

Although the Permian volcanic rocks in the Čierna Hora Mts. show geochemical characteristics similar to those of arc-related suites, palaeogeographic restorations, and geological and tectonic evidence, do not appear to support any spatial and/or temporal connection with subduction processes.

Acknowledgements: The financial support of the Slovak Research and Development Agency (projects ID: APVV-0146-16) and of the Scientific Grant Agency of the Ministry of Education of the Slovak Republic and the Slovak Academy of Sciences (project VEGA 2/0006/19) is gratefully appreciated. The authors would like to thank J. Ulrych and M. Kohút for constructive reviews and for their helpful and critical comments which led to significant improvement of an earlier version of the manuscript.

References

Arthaud F. & Matte Ph. 1977: Late Palaeozoic strike–slip faulting in southern Europe and northern Africa: results of a right-lateral shear zone between the Appalachians and Urals. *Geological Society of America Bulletin* 88, 1305–1320.

Black L.P., Kamo S.L., Allen Ch.M., Davis D.W, Aleinikoff J.N., Valley J.W., Mundil R., Campbell I.H., Korsch R.J., Williams I.S. & Foudoulis Ch. 2004: Improved $^{206}Pb/^{238}U$ microprobe geochronology by the monitoring of a trace-element-related matrix effect; SHRIMP, ID–TIMS, ELA–ICP–MS and oxygen isotope documentation for a series of zircon standards. *Chemical Geology* 205, 115–140. https://doi.org/10.1016/j.chemgeo.2004.01.003

Bonin B. 2004: Do coeval mafic and felsic magmas in post-collisional to within-plate regimes necessarily imply two contrasting, mantle and crustal, sources? A review. *Lithos* 78, 1–24. https://doi.org/10.1016/j.lithos.2004.04.042

Demko R. & Hraško Ľ. 2013: Rhyolite body Gregová near the Telgárt village (Slovakia). *Mineralia Slovaca* 45, 161–174 (in Slovak with English summary).

Dostal J., Vozár J., Keppie J.D. & Hovorka D. 2003: Permian volcanism in the Central Western Carpathians (Slovakia): Basin-and-Range type rifting in the southern Laurussian margin. *International Journal of Earth Sciences (Geol. Rundsch.)* 92, 27–35. https://doi.org/10.1007/s00531-002-0307-6

Frost B.R., Barnes C.G., Collins W.J., Arculus R.J., Ellis D.J. & Frost C.D. 2001: A geochemical classification for granitic rocks. *Journal of Petrology* 42, 2033–2048. https://doi.org/10.1093/PETROLOGY%2F42.11.2033

Gorton M.P. & Schandl E.S. 2000: From continents to island arcs: a geochemical index of tectonic setting for arc-related and within-plate felsic to intermediate volcanic rocks. *Canadian Mineralogist* 38, 1065–1073. https://doi.org/10.2113/gscanmin.38.5.1065

Hiess J., Condon D.J., McLean N. & Noble S.R. 2012: $^{238}U/^{235}U$ systematics in terrestrial uranium-bearing minerals. *Science* 335, 1610–1614. https://doi.org/10.1126/science.1215507

Hubmann B., Ebner F., Ferretti A., Kido E., Krainer K., Neubauer F., Schönlaub H.P. & Suttner T.J. 2014: The Paleozoic Era(them). *Abhandlungen der Geologischen Bundesanstalt* 66 (2nd Ed.), 9–135.

Jacko S. jr., Jacko S. sen., Labant S., Bátorová K., Farkašovský R. & Šcerbáková B. 2021: Structural constraints of neotectonics activity in the eastern part of the Western Carpathians orogenic wedge. *Quaternary International* 585, 27–43. https://doi.org/10.1016/j.quaint.2020.10.072

Jacko S. sen. 1978: Litologicko-štruktúrna charakteristika centrálnej časti pásma Čiernej Hory [Lithological-structural characteristics of the Čierna Hora Zone central part]. *Západné Karpaty: Séria Geológia* 3, 59–80 (in Slovak).

Jacko S. sen. 1985: Litostratigrafické jednotky kryštalinika Čiernej Hory [Lithostratigraphic units of the Čierna Hora crystalline basement]. *Geologické Práce, Správy* 82, 127–133 (in Slovak).

Jacko S. sen. & Rajlich P. 1973: The Alpine and pre-Alpine folds of the Čierna Hora crystalline complex. *Sborník Geologických Věd, Řada G*, Prague, 149–158.

Jacko S. sen. & Sasvári T. 1990: Some remarks to an emplacement mechanism of the Westkarpathian Paleo-Alpine nappes. *Geologický Zborník Geologica Carpathica* 41, 179–197.

Jacko S. sen., Sasvári T., Zacharov M. & Putiš M. 1995: Variscan pre-granitoid fold paragenesis of the Western Carpathians. *Krystalinikum* 22, 55–71.

Kohút M., Trubač J., Novotný L., Ackerman L., Demko R., Bartalský B. & Erban V. 2013: Geology and Re–Os molybdenite geochronology of the Kurišková U–Mo deposit (Western Carpathians, Slovakia). *Journal of Geosciences* 58, 271–282. https://doi.org/10.3190/jgeosci.150

Kotov A.B., Miko O., Putiš M., Korikovsky S.P., Salnikova E.B., Kovach V.P., Yakovleva S., Bereznaya N.G., Kráľ J. & Krist E. 1996: U/Pb dating of zircons of postorogenic acid metavolcanics and metasubvolcanics: a record of Permian–Triassic taphrogeny of the West-Carpathian basement. *Geologica Carpath*ica 47, 73–79.

Krainer K. 1993: Late- and post-Variscan sediments of the Eastern and Southern Alps. In: von Raumer J. & Neubauer F. (Eds.): Pre-Mesozoic Geology in the Alps. *Berlin-Springer*, 537–564.

Ludwig K.R. 2005: SQUID 1.12 A User's Manual. A Geochronological Toolkit for Microsoft Excel. *Berkeley Geochronology Centre Special Publication,* 1–22. http://www.bgc.org/klprogrammenu.html

Ludwig K.R. 2012: User's Manual for Isoplot 3.75. A geochronological Toolkit for Microsoft Excel. *Berkeley Geochronology Centre Special Publication* 5, 1–71. http://www.bgc.org/isoplot.html

McLennan S.M. 2001: Relationships between the trace element composition of sedimentary rocks and upper continental crust. *Geochemistry, Geophysics, Geosyst*ems 2, 2000GC000109. https://doi.org/10.1029/2000GC000109

MacLean W.H. & Barrett T.J. 1993: Lithogeochemical techniques using immobile elements. *Journal of Geochemical Exploration* 48, 108–133.

Ondrejka M., Li X-H., Vojtko R., Putiš M., Uher P. & Sobocký T. 2018: Permian A-type rhyolites of the Muráň Nappe, Inner Western Carpathians, Slovakia: In-situ zircon U–Pb SIMS ages and tectonic setting. *Geologica Carpathica* 69, 187–198.

Ondrejka M., Uher P., Putiš M., Kohút M., Broska I., Larionov A., Bojar A-V. & Sobocký T. 2021: Permian A-type granites of the Western Carpathians and Transdanubian regions: products of the Pangea Supercontinent breakup. *International Journal of Earth Sciences* 110, 2133–2155. https://doi.org/10.1007/s00531-021-02064-2

Pană D.I., Heaman L.M., Creaser R.A. & Erdmer P. 2002: Pre-Alpine crust in the Apuseni Mountains, Romania: insights from Sm–Nd and U–Pb data. *Journal of Geology* 110, 341–354. https://doi.org/10.1086/339536

Pearce J.A. 1983: The role of sub-continental lithosphere in magma genesis of destructive plate margins. In: Hawkesworth C.J. & Norry M.J. (Eds.): Continental basalts and mantle xenoliths. *Shiva*, Nantwich, 230–249.

Pearce J.A. 1996: A user's guide to basalt discrimination diagrams. In: Wyman D.A. (Ed.): Trace element geochemistry of volcanic rocks: applications for massive sulphide exploration. *Geological Association of Canada, Short Course Notes* 12, 79–113.

Pearce J.A. 2014: Immobile element fingerprinting of ophiolites. *Elements* 10, 101–108. https://doi.org/10.2113/gselements.10.2.101

Pelech O., Vozárová A., Uher P., Petrík I., Plašienka D., Šarinová K. & Rodionov N. 2017: Late Permian volcanic dykes in the crystalline basement of the Považský Inovec Mts. (Western Carpathians): U–Th–Pb SHRIMP and monazite chemical dating. *Geologica Carpath*ica 68, 6, 530–542. https://doi.org/10.1515/geoca-2017-0035

Polák M. & Jacko S. sen. (Eds.), Vozár J., Vozárová A., Gross P., Harčár J., Sasvári T., Zacharov M., Baláž B., Kaličiak M. et al. 1996: Geological map of the Branisko and Čierna Hora Mts. *Geological Survey of Slovak Republic,* Bratislava.

Polák M. (Ed.), Jacko S. sen., Vozárová A., Vozár J., Gross P., Harčár J., Zacharov M., Baláž B. et al. 1997: Explanation to the geological map of Branisko and Čierna Hora Mts., 1:50 000. *Dionýz Štúr Publ. House*, Bratislava, 1–201 (in Slovak with English summary).

Putiš M., Li J., Ružička P., Ling X. & Nemec O. 2016: U/Pb SIMS zircon dating of a rhyolite intercalation in Permian siliciclastics as well as a rhyodacite dyke in micaschists (Infratatricum, W. Carpathians). *Mineralia Slovaca* 48, 135–144.

Rojkovič I. & Konečný P. 2005: Th–U–Pb dating of monazite from the Cretaceous uranium vein mineralization in the Permian rocks of the Western Carpathians. *Geologica Carpathica* 56, 493–502.

Rudnick R.L. & Fountain D.M. 1995: Nature and composition of the continental crust – a lower crustal perspective. *Reviews of Geophysics* 33, 267–309. https://doi.org/10.1029/95rg01302

Steiger R.H. & Jäger E. 1977: Subcommission on geochronology: Convention on the use of decay constants in geo- and cosmochronology. *Earth and Planetary Science Letters* 36, 359–362.

Sun S.S. & McDonough W.F. 1989: Chemical and isotope systematic of oceanic basalts implications for mantle composition and processes. In: Sounders A.D. & Norry M.J. (Eds.): Magmatism in ocean basins. *Geological Society, London, Special Publications* 42, 313–345.

Szemerédi M., Lukács R., Varga A., Dunkl I., Józsa S., Tatu M., Pál-Molnár E., Szepesi J., Guillong M., Szakmány G. & Harangi S. 2020: Permian felsic volcanic rocks in the Pannonian Basin (Hungary): New petrographic, geochemical and geochronological results. *International Journal of Earth Sciences* 199, 101–125. https://doi.org/10.1007/s00531-019-01791-x

Tischendorf G., Förster H.-J., Gottesmann B. & Rieder M. 2007: True and brittle micas: composition and solid-solution series. *Mineralogical Magazine* 71, 285–320. https://doi.org/10.1180/minmag.2007.071.3.285

Vai G.B. 1991: Palaeozoic strike–slip rift pulses and palaeogeographer in the circum-Mediterranean Tethyan realm. *Palaeogeography, Palaeoclimatology, Palaeoecology* 87, 223–252.

Villaseñor G., Catlos E.J., Broska I., Kohút M., Hraško Ľ., Aguilera K., Etzel Th., Kyle R. & Stockli D.F. 2021: Evidence for widespread mid-Permian magmatic activity related to rifting following the Variscan orogeny (Western Carpathians). *Lithos* 390–391, 106083. https://doi.org/10.1016/j.lithos.2021.106083

Vozár J 1997: Rift-related volcanism in the Permian of the Western Carpathians. In: Grecula P., Hovorka D. & Putiš M. (Eds.): Geological evolution of the Western Carpathians. *Mineralia Slovaca, Monograph*, Bratislava, 225–234.

Vozárová A. 1979: Lithofacial characteristics of Permian in NW part of Veporicum. *Západné Karpaty: Séria Mineralógia, Petrografia, Geochémia* 6, 61–116 (in Slovak with English summary).

Vozárová A. & Vozár J. 1988: Late Paleozoic in West Carpathians. *Dionýz Štúr Institute of Geology*, Bratislava, 1–314.

Vozárová A., Konečný P., Vozár J. & Šmelko M. 2008: Upper Jurassic–Lower Cretaceous tectonothermal events in the Southern Gemeric Permian rocks deduced from electron microprobe dating of monazite. *Geologica Carpathica* 59, 89–102.

Vozárová A., Šmelko M. & Paderin I. 2009a: Permian single crystal U–Pb zircon age of the Rožňava Formation volcanites (Southern Gemeric Unit, Western Carpathians, Slovakia). *Geologica Carpathica* 60, 439–448. https://doi.org/10.2478/v10096-009-0032-1

Vozárová A., Ebner F., Kovács S., Kräutner H.G., Szederkenyi T., Krstić B., Sremac J., Aljinović D., Novak M. & Skaberne D. 2009b: Late Variscan (Carboniferous to Permian) environments in the Circum Pannonian Region. *Geologica Carpathica* 60, 71–104. https://doi.org/10.2478/v10096-009-0002-7

Vozárová A., Šmelko M., Paderin I. & Larionov A. 2012: Permian volcanics in the Northern Gemericum and Bôrka Nappe system: U-Pb zircon dating and implication to geodynamic evolution (Western Carpathians, Slovakia). *Geologica Carpathica* 63, 191–200. https://doi.org/10.2478/v10096-012-0016-4

Vozárová A., Laurinc D., Šarinová K., Larionov A., Presnyakov S., Rodionov N. & Paderin I. 2013: Pb ages of detrital zircons in relation to geodynamic evolution: Paleozoic of the Northern Gemericum (Western Carpathians, Slovakia). *Journal of Sedimentary Research* 83, 915–927. https://doi.org/10.2110/jsr.2013.66

Vozárová A., Presnyakov S., Šarinová K. & Šmelko M. 2015: First evidence for Permian-Triassic boundary volcanism in the Northern Gemericum: geochemistry and U–Pb zircon geochronology. *Geologica Carpathica* 66, 5, 375–391. https://doi.org/10.1515/geoca-2015-0032

Vozárová A., Rodionov N., Vozár J., Lepekhina E. & Šarinová K. 2016: U–Pb zircon ages from Permian volcanic rocks and tonalite of the Northern Veporicum (Western Carpathians). *Journal of Geosciences* 61, 221–237. https://doi.org/10.3190/jgeosci.215

Vozárová A., Larionov A., Šarinová K., Vďačný M., Lepekhina E., Vozár J. & Lvov P. 2018: Detrital zircons from the Hronicum Carboniferous–Permian sandstones (Western Carpathians, Slovakia): depositional age and provenance. *International Journal of Earth Sciences (Geol. Rundsch.)* 107, 1539–1555. https://doi.org/10.1007/s00531-017-1556-8

Vozárová A., Šarinová K., Laurinc D., Lepekhina E., Vozár J., Rodionov N. & Lvov P. 2019a: Exhumation history of the Variscan suture: constrains on the detrital zircon geochronology from Carboniferous–Permian sandstones (Northern Gemericum; Western Carpathians). *Geologica Carpathica* 70, 512–530. https://doi.org/10.2478/geoca-2019-0030

Vozárová A., Rodionov N., Šarinová K., Lepekhina E., Vozár J. & Paderin I. 2019b: Detrital zircon U–Pb geochronology of

Pennsylvanian-Permian sandstones from the Turnaicum and Meliaticum (Western Carpathians, Slovakia): provenance and tectonic implications. *International Journal of Earth Sciences (Geol. Rundsch.)* 108, 1793–1818. https://doi.org/10.1007/s00531-019-01733-7

Vozárová A., Šarinová K., Rodionov N. & Vozár J. 2020: Zircon U–Pb geochronology from Permian rocks of the Tribeč Mts. (Western Carpathians, Slovakia). *Geologica Carpathica* 71, 274–287. https://doi.org/10.31577/GeolCarp.71.3.6

Wang X., Griffin W.L., Chen J., Huang P. & Li X. 2011: U and Th contents and Th/U ratios of zircon in felsic and mafic magmatic rocks: improved zircon–melt distribution coefficient. *Acta Geologica Sinica (English Edition)* 85, 164–174. https://doi.org/10.1111/j.1755-6724.2011.00387.x

Wiedenbeck M., Allé P., Corfu F., Griffin W.L., Meier M., Oberli F., von Quadt A., Roddick J.C. & Spiegel W. 1995: Three natural zircon standards for U–Th–Pb, Lu–Hf, trace element and REE analyses. *Geostandards Newsletter* 19, 1–23. https://doi.org/10.1111/j.1751-908X.1995.tb00147.x

Winchester J.A. & Floyd P.A. 1977: Geochemical discrimination of different magma series and differentiation products using immobile elements. *Chemical Geol*ogy 20, 325–343. https://doi.org/10.1016/0009-2541(77)90057-2

Yuan S., Neubauer F., Liu Y., Genser J., Liu B., Yu Sh., Chang R. & Guan Q. 2020: Widespread Permian granite magmatism in Lower Austroalpine units: significance for Permian rifting in the Eastern Alps. *Swiss Journal of Geoscience* 113, 18–25. https://doi.org/10.1186/s00015-020-00371-5

Ziegler P.A. 1993: Late Palaeozoic–Early Mesozoic plate reorganization: Evolution and demise of the Variscan fold belt. In: von Raumer J.F. & Neubauer F. (Eds.): The Pre-Alpine Geology in the Alps. *Springer*, Heidelberg, 203–216.